Study of the Neuro-electrostimulation Influence on the Head Skin Capillary Blood Flow

Vladimir Kublanov, Mikhail Babich, Anton Dolganov, Evgenii Shleymovich,
Boris Zhilkin and Evgenii Plesniaev

Ural Federal University, 620002, Mira 19, Yekaterinburg, Russian Federation

Abstract: The pilot study of the 'SYMPATHOCOR-01' neuro-electrostimulation device influence on the head skin capillary blood flow is described. The infrared thermographic camera was used for the head skin capillary blood flow registration. The analysis of the registered thermograms was performed for mean head skin temperature evaluation. The experiment has shown that application of the neuro-electrostimulator in the blocking mode of the sympathetic nervous system caused the decrease of the head surface temperature. The temperature decrease is associated with the perfusion rate increase on the capillary level, which is in agreement with the neuro-electrostimulation application techniques.

1 INTRODUCTION

Many technologies of the physical fields application are aimed to improve performance of the circulatory system (Mesquita et al. 2013, Morishita et al. 2014, Yamabata et al. 2016, Jin et al. 2017). The most promising among them control the autonomic nervous system (ANS) to provide constrictive management of the blood vessels tone.

The 'SYMPATHOCOR-01' neuro-electrostimulation device is capable of performing such control. The medical techniques of the 'SYMPATHOCOR-01' device application implement the methodology of dynamic correction of the sympathetic nervous system correction (DCASNS) and provide correction of the autonomic balance, defined by the relation of the sympathetic and parasympathetic departments of the ANS (Kublanov, Shmirev, *et al.* 2010, Kublanov *et al.* 2017).

The design process of the 'SYMPATHOCOR-01' device medical application was accompanied by the experimental studies on laboratory animals (Kublanov, Danilova, *et al.* 2010, Kublanov *et al.* 2012) and the single-photon emission computed tomography imaging. (Kublanov *et al.* 2004). In clinical practice, the device has been successfully applied for treatment of the vascular dystonia; headaches of different origin, including migraine; hypertension; neurosensory hearing loss; degenera-

tive sight deficits and atrophy of the visual nerve; neurosis-like syndromes and neuropathies of the various origins (Kublanov, Shmirev, *et al.* 2010).

However, in the previous works the changes in the capillary blood flow were not studied. In most cases the capillary blood flow define the skin's temperature fluctuations. The goal of the present work is to conduct pilot study for investigation of the 'SYMPATHOCOR-01' device influence on the head skin capillary blood flow by means of the infrared thermography.

2 MATHERIALS AND METHODS

2.1 Experiment Description

The neuro-electrostimulation procedure was performed by the modern implementation of the 'SYMPATHOCOR-01' device. The key targets of the 'SYMPATHOCOR-01' devices are the neural formations in the neck region. The device is included in the register of medical equipment products of the Russian Federation – registration certificate № FCR 2007/00757.

The modern device implementation consists of two blocks. The first block is used for generation of the spatially distributed rotating field of current pulses and has two multi-element electrodes which

are placed on the neck. The first block is supplied by the built-in accumulator, has dimensions of 90 x 50 x 18.5 mm, and weighs less than 200 g. The second block is used for management and control of the neuro-electrostimulation procedure. At the moment, the second block is realized as the application for the Android operation system. Bluetooth low energy channel exchange information between the two blocks.

The pilot study was conducted in the Research Medical and Biological Engineering Centre of High Technologies, Ural Federal University. The experimental program of the study had an approval №8 from 16 October 2015 of local ethics committee in Ural State Medical University. The one relatively healthy volunteer – male, 27 years old, doesn't have any health complains – has participated in single experiment. Prior to the study volunteer has signed the participation consent. The whole experiment was supervised by the physician. The experiment layout is shown on Fig. 1.

During the whole study the volunteer was sitting on the chair. The infrared thermographic camera NEC Thermo Tracer TH9100WL was used for registration of the skin surface temperature. The infrared thermographic camera was placed on the tripod at the distance of 1.0 meter from the volunteer's head. The thermogram frame center was projected on the volunteer's forehead. In the bottom the thermogram was limited by the nose, to prevent the breathing artifacts. Example of the registered thermogram frame is shown on Fig. 2.

The camera's output was connected to the note-book, which controlled the thermograms registration and storage. The resolution of the registered thermograms was 320 x 240 pixels; 3 frames per second. The thermal resolution was 0.1°C.
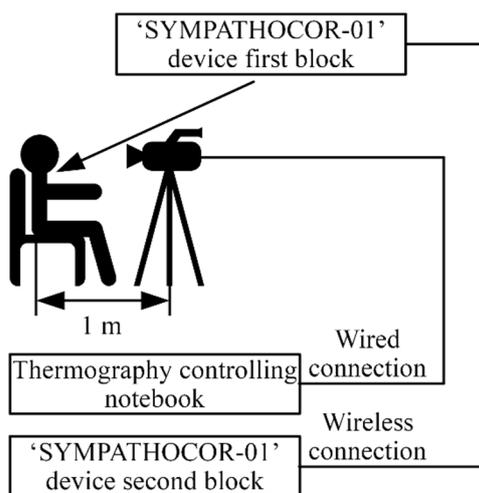
Figure 1: Experiment layout.
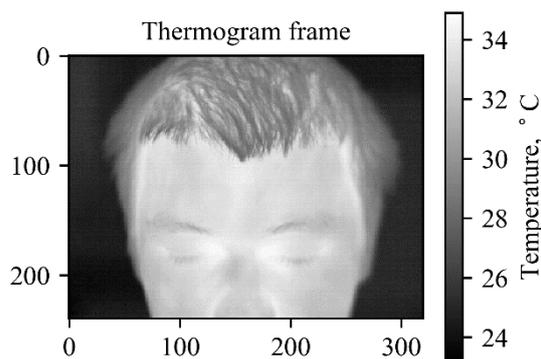
Figure 2: Thermogram frame example.

The neuro-electrostimulation device was used in the blocking mode of the Sympathetic Nervous System (SNS). For that, the following values of the biotropic field features were set: the partial impulse length – 30 us, modulation frequency – 50 Hz. The amplitude value set in a way, that volunteers had a subjective vibration feeling in the ear lobe.

2.2 Study Timeline

The pilot study consisted of 5 stages, each lasting 5 minutes:

- 1st stage – the baseline record (without neuro-electrostimulation);
- 2nd stage – stimulation of the left neck ganglion of the SNS;
- 3rd stage – rest (without neuro-electrostimulation);
- 4th stage – stimulation of the right neck ganglion of the SNS;
- 5th stage – aftereffect (without neuro-electrostimulation).

The thermogram frames were registered during the whole study. The whole study data was stored as 4500 *.csv files, each containing information about single thermogram frame.

2.3 Thermogram Frame Processing

The block-diagram of the thermogram processing is presented on Fig. 3.

The processing algorithm is a cycle; each cycle iteration process single thermogram frame. At the first step, the next thermogram frame is selected. On the second step, the threshold temperature value ($T_{threshold}$) is evaluated. For the $T_{threshold}$ evaluation the histogram distribution of the thermogram frame is analyzed. The histogram of the thermogram frame, shown on Fig. 2, is presented on Fig. 4.
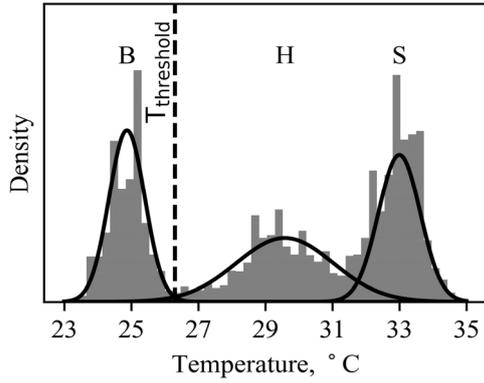
Figure 4: Thermogram frame histogram.
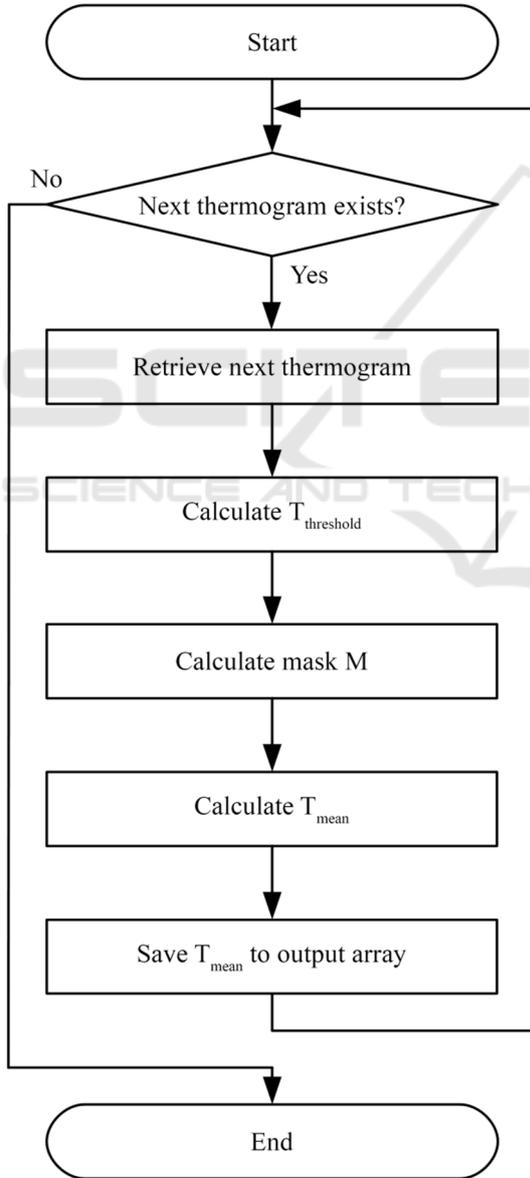
Figure 3: Thermogram processing block-diagram.

Histogram, presented on Fig. 4, has a polymodal distribution. Each thermogram frame consists of three normal distributions, they are B – background tempe-rature, H – hair temperature and S – skin temperature. The expectation maximization algorithm is used to evaluate the probability densities of each distribution (Moon 1996). The equality temperature of probability densities for distributions B and H was used as the $T_{threshold}$.

On the third step of the iteration the mask M is constructed using the $T_{threshold}$ value. For each horizontal (x) and vertical (y) indexes of the original thermogram each element of M is defined as followed:

$$M_{x,y} = \begin{cases} 1, if\ T_{x,y} > T_{threshold} \\ 0, otherwise \end{cases} \qquad (1)$$

The mask allows separating image of the head from the background. The mask, constructed for the thermogram frame, shown on Fig. 2, is presented on Fig. 5.
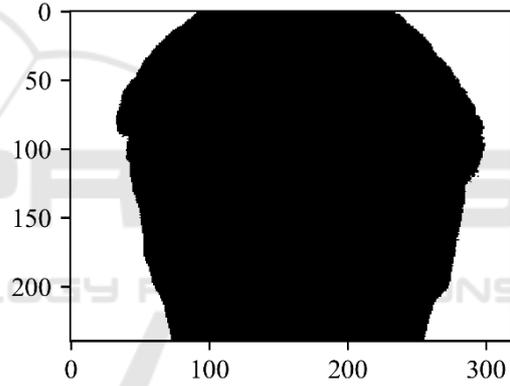
Figure 5: Thermogram frame mask.

On the fourth step of the iteration, the mean temperature value of the head is evaluated in accordance with the following formula:

$$T_{mean} = \frac{\sum_{x,y} M_{x,y} \circ T_{x,y}}{\sum_{x,y} M_{x,y}} \qquad (2)$$

On the fifth iteration step the T_{mean} value is saved to the output array.

The algorithm was written on Python 3.6.0 with Anaconda 4.3.1 distribution. As the result of the algorithm running, the plot of the mean temperatures for all thermogram frames was created.

3 RESULTS AND DISCUSSION

The human body thermoregulation is organized by the variety of the physical process that includes
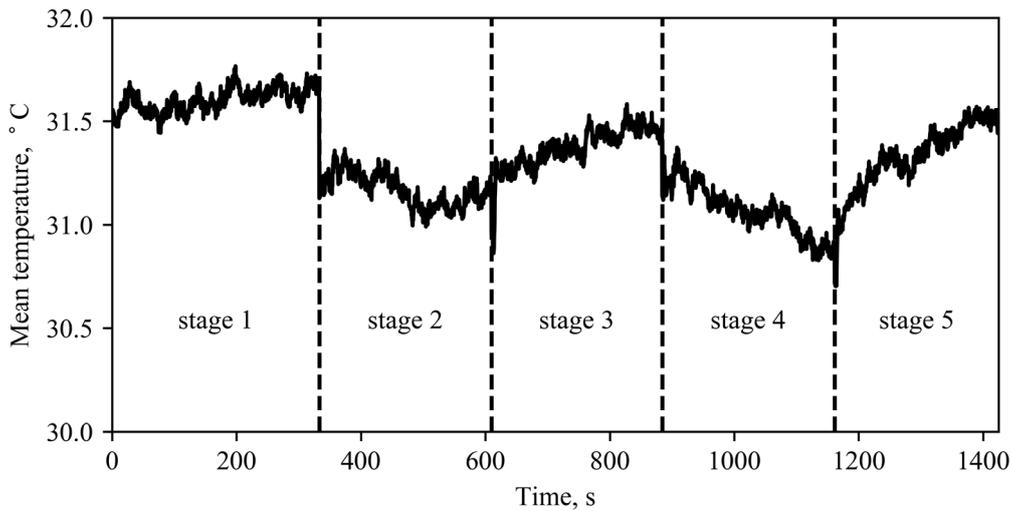
Figure 6: Mean temperature plot for whole study timeline.

metabolic heat generation, change of the thermal insulation features of the tissues and sweating. One of the metabolic heat production components is the non-contracting thermogenesis. The short-term control of the non-contracting thermogenesis is done through the ANS. The suppression of the nervous system activity leads to the decrease of the non-contracting thermogenesis. The temperature regulation effects, which are associated with the blood supply, vary for different functional areas. For the human head there are two types of the functional areas: acral areas, which includes hears, lips and nose. The second type includes the remaining skin surface of the head (Hensel et al. 1973).

The blood suply of the acral areas is controlled by the noradrenalin sympathetic nerves. Increase of the sympathetic tone causes shrinking of the vasculars. Shrinked vasculars significantly deacrease convention.

The sweating process is only regulated through the holinergetic sympathetic fabrics. The blocking of the holinergetic synapsis results in the sweating decrease, which, in turn, increase body temperature.

The heat distribution in living organism tissues is described by the Pennes bio-heat equation (Bergman and Incropera 2011):

$$\rho c \frac{\partial T}{\partial t} = \nabla(k\nabla T) + \omega_b c_b (T_a - T) + q_m \qquad (3)$$

where: ρ – density of the biological tissue, c – heat capacity of the biological tissue, k – thermal conduction of the biological tissue. ω_b –mass blood flow per unit volume of the biological tissue, c_b – blood heat capacity, q_m – metabolic heat per unit volume of the biological tissue, T_a – arterial blood

temperature, T – biological tissue temperature, $\partial T/\partial t$ – temperature variation rate.

According to the Pennes equation the temperature of the biological tissue is defined by three components: heat exchange with the surrounding biological tissues $\{\nabla(k\nabla T)\}$, heat exchange with the blood $\{\omega_b c_b (T_a - T)\}$, metabolic heat of the tissue - q_m.

Mean temperatures plot for all thermogram frames, with annotated experiment stages is shown on figure 6. The plot shows, that mean temperature of the head surface decreases during the 2nd and 4th stages – neuro-electrostimulation stages. The difference between the time-averaged temperature of the first and second stage was 0.44 °C. The difference between the time-averaged temperature of the first and the fourth stage was 0.53 °C.

The measuring accuracy of the thermal imager was ±2% or 2°C, but the thermal resolution was 0.04°C (Gerlach 2006). Therefore, changes on the 0.44°C and 0.53°C are not associated with the noise of thermal imager. These changes reflect metabolic reaction of the subject.

The neuro-electrostimulation device was working in the blocking mode of SNS activity. Therefore, stimulation decreases the vascular tone and, as the results improves perfusion rate in tissues. In accordance with the Pennes equation, in particular the second component $\{\omega_b c_b (T_a - T)\}$, the skin surface should decrease, on the other hand, the blocking of the SNS activity leads to the non-contracting thermogenesis (the q_m component). Jointly, it results in the general decrease of the head skin temperature.

When the stimulation process is stopped – stages 3 and 5 – blood perfusion and non-contracting thermogenesis tends to return to the original values.

This results in the graduate increase of the temperature to the baseline values.

One can note the different behavior of the thermal changes in the stages 2 and 4. It can be associated with the different organization of the left and right upper ganglia.

4 CONCLUSIONS

Presented in the paper results show that neuro-electrostimulation of the neck neural conducting path allows one to regulate skin capillary blood flow of the head and, as the result, to change skin temperature. If the blocking mode of the sympathetic nervous system is selected than it is possible to decrease skin temperature. It was hypothesized that this physical phenomena is define by the changes of the blood perfusion and decrease of the non-contracting thermogenesis

The development of the described in this work methodology can result in application of the 'SYMPATHOCOR-01' neuro-electrostimulation for treatment of the skin defects, burns and in cosmetic tasks by means of the blood flow control.

REFERENCES

Bergman, T. L. and Incropera, F. P., 2011. *Introduction to heat transfer*. John Wiley & Sons.

Gerlach, N., 2006. Comparison of Thermal Imaging Systems Used in Thermography as a Non Destructive Testing Method for Composite Parts. *In*: *European Conference on Nondestructive Testing, ECNDT 2006 Proceedings, Tu*. 25–29.

Hensel, H., Bruck, K., and Raths, P., 1973. Homeothermic organisms. *Temperature and life. Springer, Berlin Heidelberg New York*, 502–761.

Jin, H.-K., Hwang, T.-Y., and Cho, S.-H., 2017. Effect of Electrical Stimulation on Blood Flow Velocity and Vessel Size. *Open Medicine*, 12, 5–11.

Kublanov, V. S., Babich, M., and Dolganov, A., 2017. Principles of Organization and Control of the New Implementation of the 'SYMPATHOCOR-01' Neuro-electrostimulation Device. *In*: *BIOSIGNALS*. 276–282.

Kublanov, V. S., Danilova, I. G., Goette, I. F., Brykina, I. A., and Shaljagin, M. A., 2010. Spatially Distributed Field of Electric Impulses for Regeneration of Ishemic Muscules. *Biomedical Radioelectronics*, (10), 34–39.

Kublanov, V. S., Lavrova, S. A., Shershever, A. S., Telegin, A. V., and Shmikalov, V. A., 2004. Lechenie epilepsii s primeneniem prostranstvenno raspredelennich vrashayushichsya poley impulsov toka [epilepsy treatment by means of the spatially distributed rotating fields of current pulses]. *Biomedical Radioelectronics*, (5–6), 4–15.

Kublanov, V. S., Porshnev, S. V., Danilova, I. G., Goette, I. F., Levashkina, A. O., and Syskov, A. M., 2012. Experimental modeling of the effects of autonomic regulation in the correction of immobilization stress rats. *Biomedical Radioelectronics*, (8), 56–67.

Kublanov, V. S., Shmirev, V. I., Shershever, A. S., Kazakov, J. E., and others, 2010. About Innovative Possibilities of Device 'SIMPATOCOR-01' in Management of Functional Disorders of Vegetative and Central Nervous System in Neurology, Kremljovskaya Medicine. *Clinichesky Vestnik*, 4, 60–64.

Mesquita, R. C., Faseyitan, O. K., Turkeltaub, P. E., Buckley, E. M., Thomas, A., Kim, M. N., Durduran, T., Greenberg, J. H., Detre, J. A., Yodh, A. G., and Hamilton, R. H., 2013. Blood flow and oxygenation changes due to low-frequency repetitive transcranial magnetic stimulation of the cerebral cortex. *Journal of Biomedical Optics*, 18 (6), 067006.

Moon, T. K., 1996. The expectation-maximization algorithm. *IEEE Signal Processing Magazine*, 13 (6), 47–60.

Morishita, K., Karasuno, H., Yokoi, Y., Morozumi, K., Ogihara, H., Ito, T., Fujiwara, T., Fujimoto, T., and Abe, K., 2014. Effects of Therapeutic Ultrasound on Intramuscular Blood Circulation and Oxygen Dynamics. *Journal of the Japanese Physical Therapy Association*, 17 (1), 1–7.

Yamabata, S., Shiraishi, H., Munechika, M., Fukushima, H., Fukuoka, Y., Hojo, T., Shirayama, T., Horii, M., Matoba, S., and Kubo, T., 2016. Effects of electrical stimulation therapy on the blood flow in chronic critical limb ischemia patients following regenerative therapy. *SAGE Open Medicine*, 4.